Spin dynamics and magnetic phase diagram of $La_{1-x}Ca_xMnO_3$ ($0 \leqslant x \leqslant 0.15$)

R. Laiho,* E. Lähderanta, and J. Salminen
Wihuri Physical Laboratory, Department of Physics, University of Turku, FIN-10014 Turku, Finland

K. G. Lisunov and V. S. Zakhvalinskii
Institute of Applied Physics, Academiei Str. 5, MD-2028 Kishinev, Moldova

(Received 24 April 2000; revised manuscript received 6 November 2000; published 29 January 2001)

Spin dynamics of ceramic $La_{1-x}Ca_xMnO_3$ with $x=0$, 0.05, and 0.15 and the relative Mn^{4+} concentration $c=0.18-0.22$ is investigated by measurements of the ac susceptibility and the relaxation of the thermoremanent magnetization (TRM). The $\chi_{ac}(T)$ function exhibits a transition from the paramagnetic to a mixed spin-glass and ferromagnetic phase. Below that is found a steep decrease and onset of the frequency dependence of $\chi_{ac}(T)$, providing evidence for existence of a reentrant spin glass (RSG) phase. The dependence of the spin-glass freezing temperature, T_f, on f satisfies the conventional critical slowing-down law, $\tau/\tau_0 = (T_f/T_G - 1)^{-zv}$ with $\tau = 1/f$, $zv = 12 \pm 2$, $\tau_0 \sim 10^{-12}$ s and the glass temperature, T_G, decreasing from 93 to 70.5 K when x is increased from 0 to 0.15. The relaxation rate $S(t)$ of TRM has a clear maximum near a wait time $t_w \sim (2-4) \times 10^3$ s and the function $S(T)$ shows a sharp maximum near T_G. The plots of $S(T)$ exhibit a substantial decrease at $T > T_G$ while for $T < T_G$ they collapse into a single curve, as typical for mixed ($T_G < T < T_C$) and RSG phases, respectively. The observed spin dynamics agrees completely with the magnetic phase diagram (paramagnetic, mixed, and RSG phases with decreasing T) predicted recently for a system containing lattice disorder and competing superexchange and double exchange interactions.

DOI: 10.1103/PhysRevB.63.094405 PACS number(s): 75.50.Lk, 75.90.+w

Manganite perovskite alloys $La_{1-x}Ca_xMnO_3$, briefly LCMO, have attracted considerable attention due to the colossal magnetoresistance appearing near the paramagnetic (PM) to ferromagnetic (FM) transition temperature, T_C.[1] Belonging to the class of mixed-valence materials they demonstrate a variety of interesting electronic and magnetic properties which are determined by the ratio of the Mn^{4+} and Mn^{3+} ion concentrations, c. Namely, for $c < 0.15-0.20$ they form an insulating antiferromagnetic (AFM) state below a Neel temperature T_N and a metallic FM phase for $0.15-0.20 < c < 0.5$ and $T < T_C$.[2,3] Canted AFM spin orientation is observed below T_N or T_C for $c = 0-0.1$,[4] while near $c \approx 0.5$ charge ordered structure is found.[5] These properties can be explained by competition between the Mn^{3+}–Mn^{3+} superexchange (SE) interaction, leading to the AFM ordering, and the double-exchange (DE) mechanism aligning the Mn^{3+}–Mn^{4+} spins ferromagnetically by electron transfer via O^{2-} ions.[6] On the other hand, as found in recent extensive investigations, magnetic properties of LCMO and related perovskite compounds are not restricted only to those mentioned above. In neutron-scattering experiments existence of droplets with magnetic coupling different from the matrix has been established in the FM phase of LCMO (Ref. 7) and evidence of small FM clusters or polarons in the PM phase of $La_{0.67}Sr_{0.33}MnO_3$ (Ref. 8) and in $La_{0.75}Ca_{0.2}Mn(Co)O_3$ (Ref. 9) has been obtained. In $La_{0.8}Ca_{0.2}Mn(Co)O_3$ it was found that upon approaching T_C from the low-temperature side the FM phase breaks down into small superparamagnetic clusters with size of ~5–10 nm.[10] From investigations of local properties of $(La_{1-x}Tb_x)_{2/3}Ca_{1/3}MnO_3$ by muon spin relaxation and neutron diffraction experiments it was concluded that both spin-glass (SG) and cluster-glass (CG) phases exist in this compound.[11] Existence of a CG phase has been reported also for the novel pyroclore material $Tl_{2-x}Bi_xMn_2O_7$ where it was attributed to localized magnetic polarons of size 1–1.5 nm.[12] Recent electrical transport measurements give evidence of small polaron contribution to electrical conductivity in the metallic FM state of LCMO epitaxial films.[13]

Besides the phase separation effects mentioned above, irreversible dc magnetic phenomena have been observed in different manganite and cobaltite perovskites in low fields (see, e.g., Refs. 14–16) suggesting a frustrated magnetic ground state, although the nature of the frustration remains still controversial. It might be attributed to magnetic nanoparticles (spin polarons or hole rich droplets) distributed randomly in the lattice or exhibiting a wide size distribution. On the other hand, the frustration can result from lattice disorder of interatomic scale due to the presence of competing SE–DE interactions.[17] Really, in LCMO the Mn^{4+} ions are distributed in random up to the charge ordered state at $c \approx 0.5$. Therefore, the interactions between the Mn ions can be frustrated due to any fluctuations of the density of Mn^{4+} in the matrix. Additionally, one cannot exclude the possibility that the character of the frustration may differ even in the same material in different intervals of composition[14] or in samples prepared by different methods.

In dc magnetization measurements of ceramic LCMO with $x=0-0.4$, all samples exhibited below T_C magnetic irreversibility shown by deviation of the zero-field cooled dc susceptibility, χ_{ZFC}, from the field-cooled susceptibility χ_{FC}.[18] However, distinct differences have been observed between the groups of samples with $x < x_b$ ($c < c_b$) and $x > x_b$ ($c > c_b$) where $x_b \approx 0.18$ and $c_b \approx 0.23$.[14,19] Namely, the samples of the first group exhibit a clear second-order FM transition at T_C with the value of the critical exponent $\gamma = 1.2$ lying between those of the mean field theory

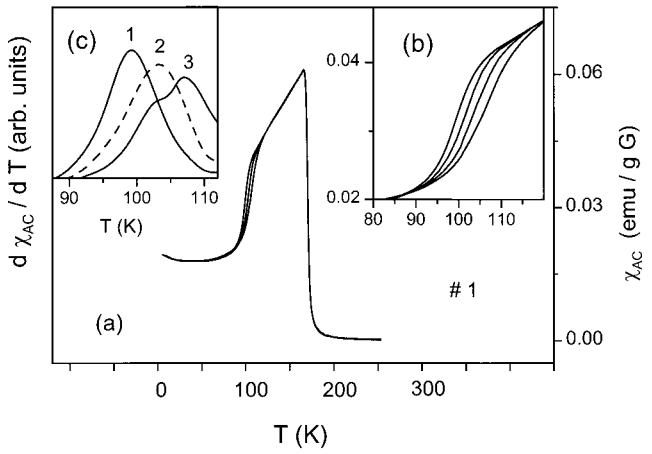

FIG. 1. Dependence of χ_{ac} on temperature for the sample #1 at $f=0.25$, 4, and 40 Hz (from up to down) (a). A part of the curve χ_{ac} (T) in an enlarged scale for $f=0.25$, 1.5, 8, and 40 Hz (from up to down) (b). Temperature dependence of $d\ \chi_{ac}(T)/dT$ for $f=0.25$ Hz (1), 4 Hz (2), and 40 Hz (3) for the sample #1 (c).

($\gamma=1$) and of the three-dimensional (3D)-Heisenberg model ($\gamma=1.4$), which agrees well with the literature data.[20–22] The samples of the second group also demonstrate a critical behavior near T_C, but with another value of $\gamma=1.64$. Moreover, independent analysis of the modified Arrot plots of LCMO and related compounds demonstrated that the FM transition in these samples may even be of the first order.[20] Next, in the samples of the first group was observed below T_C the relation $\chi_{FC}(B)-\chi_{ZFC}(B)=\mathrm{TRM}/B$, where TRM is the thermoremanent magnetization. This is typical for SGs. In the samples of the second group deviations from this relation suggest a transition to a CG phase.[19] At last, all samples of the first group demonstrate between $T\sim 70-100$ K an additional magnetic transition visible as a steep decrease of χ_{ZFC} when T is decreased, what does not take place in the second group samples.[18]

In this paper we present measurements of the ac susceptibility and relaxation of TRM in LCMO with $x\leqslant 0.15$, giving evidence for existence of a low-temperature mixed (FM+SG) or M phase and a reentrant spin-glass (RSG) phase.

The samples of cubic LCMO were synthesized with the standard ceramic technique.[18] From dc magnetic measurements the values of $c=0.21$, 0.18, and 0.22 and $T_C=172$, 173, and 190 K were determined for the samples with $x=0$, 0.05, and 0.15, denoted below by #1, #2, and #3, respectively.[18] The deviation of c from the corresponding values of x is connected with formation of vacancies in the metallic sublattice during sample preparation. The measurements of the ac susceptibility $\chi_{ac}(T,f)$ were made in zero dc field between $T=5-300$ K and $f=0.25-40$ Hz, using a SQUID magnetometer. The amplitude of the ac field was 1 G. For investigations were chosen only samples of the first group exhibiting a clear second-order FM transition, an additional low-temperature magnetic transition and typical SG-like behavior in dc magnetic field. It is important to note, also, that the samples chosen have very close values of c what allows to exclude or minimize the variation of their properties connected with charge degrees of freedom.

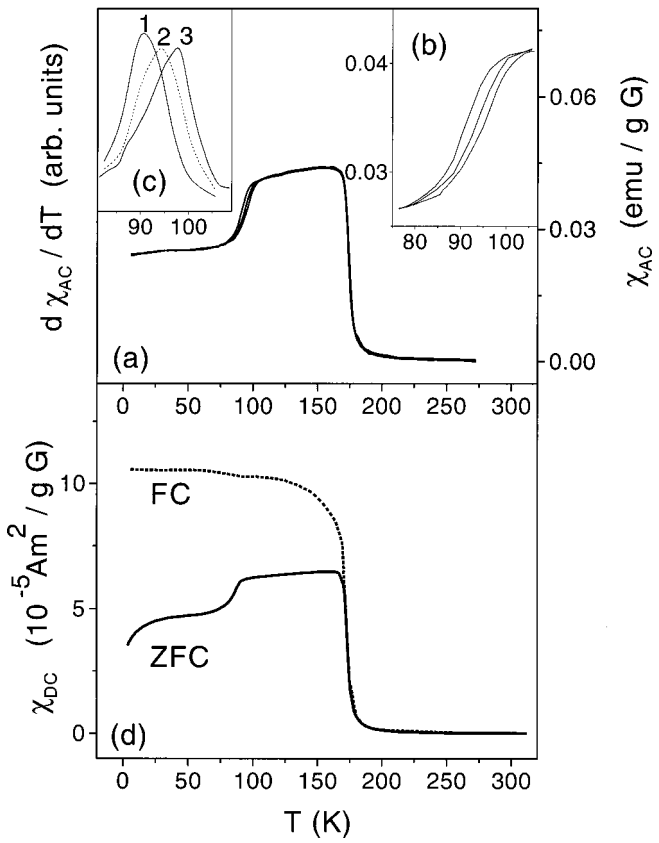

FIG. 2. Dependence of χ_{ac} on temperature for the sample #2 at $f=0.25$, 4, and 22 Hz (from up to down) (a). A part of the curve $\chi_{ac}(T)$ in an enlarged scale for $f=0.25$, 4, and 40 Hz (from up to down) (b). Temperature dependence of $d\ \chi_{ac}(T)/dT$ for $f=0.25$ Hz (1), 4 Hz (2), and 40 Hz (3) (c). Temperature dependence of the static magnetic susceptibility χ_{dc} measured in the field of 2 G (d).

As shown in Figs. 1(a)–1(b) the behavior of $\chi_{ac}(T)$ with decreasing T for the sample #1 is similar to that of $\chi_{ZFC}(T)$,[18] including the FM transition at the same value of T_C (171 K), a shoulder and a steep decrease with the inflection point at the freezing temperature $T_f\sim 100$ K and a weak variation down to the lowest T. The values of $\chi_{ac}(T)$ depend on f between 120 K and 90 K, but with further decrease of the temperature the frequency dependence vanishes. When f is increased T_f shifts to higher values [see Fig. 1(c)].

As evident from Figs. 2(a)–2(c), the behavior of $\chi_{ac}(T,f)$ for the sample #2 is similar to the sample #1, except an almost flat interval between the FM transition and the steep decrease and onset of the frequency dependence of $\chi_{ac}(T)$. With further increase of x (sample #3, not shown) the shoulder on $\chi_{ac}(T)$ is restored, the shape of the function $\chi_{ac}(T,f)$ resembles that of #1, excluding higher T_C(193 K), a 2 times lower absolute value of χ_{ac} and about 20 K lower T_f. The downward concave anomaly in the FC$\chi_{dc}(T)$ curve below 100 K and the shoulder in the ZFC$\chi_{dc}(T)$ curve shown in Fig. 2(d), are signatures of an FM to RSG transition.[26,27]

The behavior of $\chi_{ac}(T,f)$ observed in this work as compared with that of the dc magnetization (deviation of

$\chi_{ZFC}(T)$ form $\chi_{FC}(T)$ just below T_C)[18,19] suggests a coexistence of FM and SG phases (the M phase) between T_C and T_f and a transition into a low-temperature RSG state below T_f. Both the M and the RSG phases have been predicted for a system containing competing SE and DE, interactions and lattice disorder.[17] A similar conclusion, coexistence of glassy and FM phases was made recently from investigations of ac susceptibility in $La_{0.5}Sr_{0.5}CoO_3$.[15] Additionally, coexistence of two spatially separated phases with different Mn-ion spin dynamics has been found by muon spin relaxation and neutron spin echo measurements in $La_{0.7}Ca_{0.3}MnO_3$ over the temperature range of $0.7\,T_C \leqslant T \leqslant T_C$.[23] However, there are distinct differences with the behavior observed in Refs. 15 and 23 and our data. First, we point out that the steep decrease of $\chi_{ac}(T)$ and $\chi_{ZFC}(T)$ found with lowering of T in LCMO having $x \leqslant 0.15$ does not take place in $La_{0.5}Sr_{0.5}CoO_3$.[15] Another important feature is that the onset of the frequency dependence of $\chi_{ac}(T)$ takes place definitely below T_C and simultaneously with that of the steep decrease of $\chi_{ac}(T)$, which is in a striking difference with the behavior of $\chi_{ac}(T)$ in $La_{0.5}Sr_{0.5}CoO_3$.[15] The samples with $x \geqslant 0.2$ do not exhibit a second magnetic transition or a low-temperature inflection of $\chi_{ZFC}(T)$ at all, and belong to the second group of samples with different dc magnetization properties (see above). Therefore, the coexistence of two different phases found in $La_{0.7}Ca_{0.3}MnO_3$ (Ref. 23) can exist in LCMO with $x \geqslant 0.2$ but should break down with lowering of T in the samples with $x \leqslant 0.15$.

Evidence of the RSG state in our samples is obtained from analysis of the frequency dependence of T_f. In spin-glasses the dependence of $T_f(f)$ is connected with divergence of the maximum relaxation time of the system as T approaches T_f from the high-temperature side. According to conventional spin-glass dynamics the relaxation time τ (or the inverse excitation frequency f^{-1}) diverges as[24]

$$\tau/\tau_0 = (T_f/T_G - 1)^{-z\nu}, \tag{1}$$

where τ_0 is the shortest relaxation time available to the system; T_G is the SG temperature determined by the interactions in the system; z is the dynamic critical exponent; and ν is the critical exponent of the correlation length. Typical values of τ_0 lie between 10^{-12}–10^{-14} s for both PM–SG and FM–RSG transitions, i.e., of order of the spin-flip time of atomic magnetic moments (see, e.g., Refs. 25–27). It has been proposed that the FM–RSG transition may also be governed by an activated dynamic scaling behavior[26]

$$\ln(\tau/\tau_0) = (T_G/T_f)(T_f/T_G - 1)^{-\psi\nu}, \tag{2}$$

where ψ is another critical exponent. Sometimes the dynamics of a SG transition is described by the Vogel–Fulcher law[28]

$$\tau/\tau_0 = \exp[E_a/k(T_f - T_G)], \tag{3}$$

determined by the activation energy E_a. Below, we use Eqs. (1)–(3) to analyze the frequency dependence of T_f in Fig. 3.

To simplify the analysis of $T_f(f)$ with Eq. (1), the relations between the parameters τ_0, $z\nu$, and T_G can be obtained, allowing two of them to be excluded from the fitting

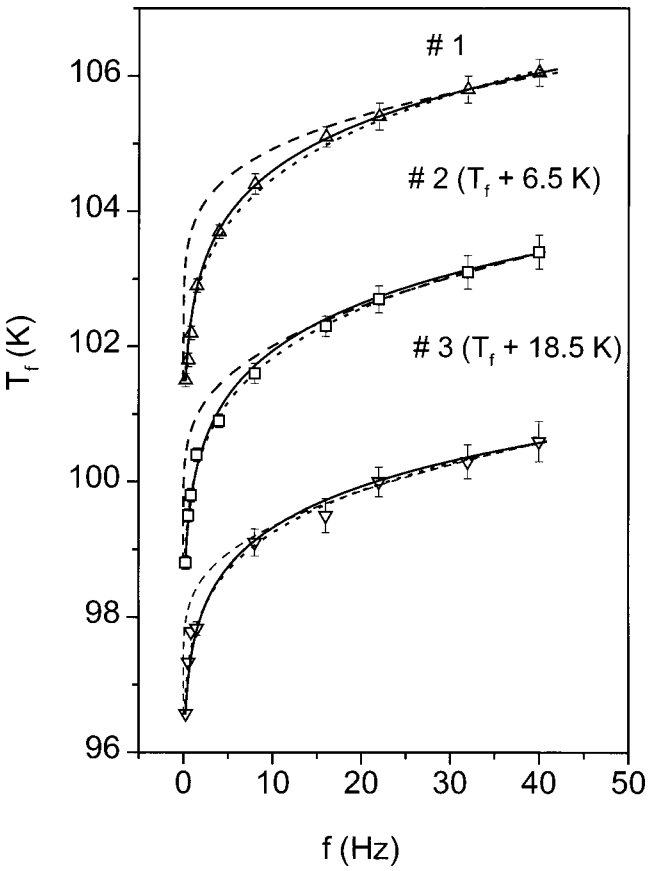

FIG. 3. Measured values (symbols) and plots of $T_f(f)$ evaluated from Eq. (1) (solid line), Eq. (2) (dotted line), and Eq. (3) (dashed line) as described in the text. The data for the samples #2 and #3 are shifted for convenience.

procedure as follows. If f_1 is the minimum and f_2 the maximum frequency used in the measurements (in our case, $f_1 = 0.25$ Hz and $f_2 = 40$ Hz), $T_1^* = T_f(f_1)$ and $T_2^* = T_f(f_2)$, then, integrating the left- and the right-hand side of Eq. (1) over f in the interval of (f_1, f_2) and over T_f in the interval of (T_1^*, T_2^*), we obtain after some algebra

$$T_G = \frac{T_2^* \ln f_2 - T_1^* \ln f_1 - C_{12} - (T_2^* - T_1^*) z\nu}{\ln(f_2/f_1)} \tag{4}$$

and

$$\tau_0 = \left[\frac{D_{12} - T_G \ln(f_2/f_1)}{z\nu (f_2^{1/z\nu} - f_1^{1/z})} \right]^{z\nu} \tag{5}$$

In these equations, $C_{12} = \int_{T_1^*}^{T_2^*} \ln f dT_f$ and $D_{12} = \int_{f_1}^{f_2} T_f d \ln f$ are the parameters that can be easily evaluated by numerical integration of the corresponding curves. Therefore, by introducing C_{12} and D_{12}, the parameters τ_0 and T_G can be excluded using Eqs. (4) and (5), and $z\nu$ can be determined by fitting the experimental data of T_f with Eq. (1). For Eq. (2) or (3), only one of the parameters T_G, τ_0, and $\psi\nu$ (or T_G, τ_0, and E_a, respectively) can be excluded in a similar way,

without any ambiguity or mutual dependence between the two others.

In Fig. 3 are shown the fits of Eqs. (1) (solid line), (2) (dotted line), and (3) (dashed line) with experimental data of $T_f(f)$. We find a good agreement between the observed values and the critical slowing down Eq. (1) with $z\nu = 12 \pm 2$ in all the investigated LCMO specimens. These values are also very close to $z\nu = 11.8$ obtained in SG $Ho_5Co_{50}Al_{45}$ (Ref. 29) and $z\nu = 12.0-14.6$ found in RSG $Pd_9Co_{50}Al_{41}$,[25] but are higher than in the RSG $(Fe_{0.2}Ni_{0.8})_{75}P_{16}B_6Al_3$ ($z\nu \approx 8$).[26] The values of T_G obtained with Eq. (1) vary from 93 K (sample #1) to 70 K (sample #3). Only the order of the magnitude of $\tau_0 \sim 10^{-12}$ s can be determined with the method used above. However, it is possible to conclude that τ_0 given by Eq. (1) lies much closer to relaxation times of atomic scale moments ($\sim 10^{-13}$ s) than to values typical for noninteracting magnetic nanoclusters [$\tau_0 \sim 10^{-9}-10^{-10}$ s (Refs. 30–32)]. It is natural to suppose that possible interactions between the magnetic nanoparticles (which can exist in LCMO, see above) would not change τ_0, significantly. Therefore, it is likely that the value of $\tau_0 \sim 10^{-12}$ s found with Eq. (1) for $x = 0-0.15$ reflects frustration stemming, in the presence of the competing SE–DE interactions, rather from lattice disorder of the interatomic scale[17] than from formation of magnetic nanoparticles.

As can be seen from Fig. 3, the fit of $T_f(f)$ with Eq. (2) is practically of the same quality as that of Eq. (1). Also the values of T_G are the same (within the error) as those obtained with Eq. (1). Equal values of the exponent $\psi\nu = 1.4 \pm 0.3$ are found in all samples. However, Eq. (2) yields $\tau_0 \sim 10^{-5}-10^{-6}$ s which is too long to characterize the dynamics of any frustrated system.[25–27] The worst fit is obtained with Eq. (3) which requires even longer $\tau_0 \sim 10^{-4}-10^{-5}$. The values of T_G found with Eq. (3) are ~9–10 K higher than obtained with Eqs. (1) and (2). On the other hand, those of $E_a = 40.5$, 21.5, and 17.6 K for samples #1, #2, and #3, respectively, exhibit too rapid decrease with x. To summarize, only Eq. (1) provides a satisfactory description of our $T_f(f)$ data, demonstrating a critical slowing down behavior typical for RSGs.

Time-dependent TRM relaxation measurements were made to get information about the ageing effect. For investigations of the time decay of TRM the sample was first cooled in the field of 50 G from the room temperature down to the measuring temperature. After a wait time, $t_W \sim (2-4) \times 10^3$ s, the field was abruptly reduced to zero and the decay of TRM was recorded over a time period of 10^4 s.

In Fig. 4(a) is shown the relaxation of TRM over a time scale of 10^4 s for samples #1–#3 after the wait times $t_W = 1.8$, 3.4, and 3.5×10^3 s, respectively. The corresponding relaxation rates, $S = -d\ \mathrm{TRM}/d \log t$, are plotted in Fig. 4(b). The plots of TRM vs $\log t$ have an inflection point when the observation time nearly equals t_W and the relaxation rates attain a corresponding maximum. This is a signature of the ageing behavior[25–27] in all the investigated samples. The temperature dependence of S for the observation time $t = 10^3$ s, chosen near the maximum of $S(t)$, is shown in Fig. 4(c). It is found that $S(T)$ attains a maximum

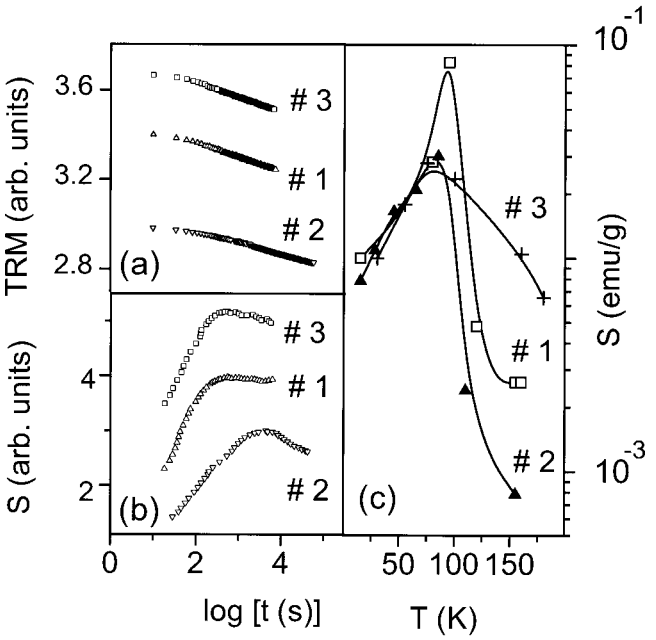

FIG. 4. Dependencies of TRM (a) and S (b) on $\log t$ for the samples #1 at 80 K, #2 at 65 K, and #3 at 75 K, measured after the wait time $t_w = 1.8 \times 10^3$, 3.4×10^3, and 3.5×10^3 s, respectively. Dependence of the relaxation rate S on T at $t = 10^3$ s. The solid lines are guides for the eye.

near T_G and drops for $T > T_G$ by more than one order of the magnitude in the samples #1 and #2 and decreases substantially but less steeply in the sample #3. For $T < T_G$ the plots of $S(T)$ collapse into a single curve. Such behavior of $S(T)$ supports the conclusion about existence of the M phase between T_C and T_G, where the magnetic order is violated, and the RSG phase below T_G. The collapse of $S(T)$ at $T < T_G$ implies that a common reason of frustration leads to the RSG phase in all our samples.

In conclusion, dynamic magnetic properties are investigated in $La_{1-x}Ca_xMnO_3$ with $x = 0$, 0.05, and 0.15 and $c = 0.18-0.22$. In all samples, a transition into a mixed (FM+SG) phase is observed at T_C, in agreement with dc magnetic measurements.[18,19] A clear transition to a RSG state at $T_f < T_C$ is identified by a steep decrease of $\chi_{ac}(T)$ with lowering the temperature, accompanied by onset of a dependence of χ_{ac} on f. The frequency dependence of the freezing temperature $T_f(f)$ can be well described with the conventional critical slowing-down law given by Eq. (1) with $z\nu = 12 \pm 2$, $\tau_0 \sim 10^{-12}$ s and the glass temperature T_G decreasing when x is increased. The ageing effect is observed in all the samples for time scales up to 10^4 s and the relaxation rate $S(t)$ reaches a maximum near a wait time $t_W \sim (2-4) \times 10^3$ s. The function $S(T)$ attains a sharp maximum near T_G and decreases steeply at $T > T_G$. Below T_G the plots of $S(T)$ collapse into a single curve, reflecting a sequence of transitions to the mixed and then to the RSG state when T is decreased. The observed spin dynamics of LCMO with $x = 0-0.15$ and $c = 0.18-0.22$ agrees completely with the phase diagram predicted for a system containing competing SE–DE interactions and lattice disorder.[17]

*Electronic address: erlah@utu.fi

[1] R. von Helmolt, J. Wecker, B. Holzapfel, L. Schulz, and K. Sammer, Phys. Rev. Lett. **71**, 2331 (1993).
[2] E. O. Wollan and W. C. Koehler, Phys. Rev. **100**, 545 (1955).
[3] P. Schiffer, A. P. Ramirez, W. Bao, and S.-W. Cheong, Phys. Rev. Lett. **75**, 3336 (1995).
[4] F. Moussa, M. Hennion, G. Biotteem, J. Rodriguez-Carvajal, L. Pinsard, and A. Revcolevschi, Phys. Rev. B **60**, 12 299 (1999).
[5] C. H. Chen and S.-W. Cheong, Phys. Rev. Lett. **76**, 4042 (1996).
[6] P.-G. de Gennes, Phys. Rev. **118**, 141 (1960).
[7] M. Hennion, F. Moussa, G. Biotteau, J. Rodriguez-Carvajal, L. Piusard, and A. Revcolevschi, Phys. Rev. Lett. **81**, 1957 (1998).
[8] J. W. Lynn, R. W. Ervin, J. A. Borchers, Q. Huang, A. Santoro, J.-I. Peng, and Z. Y. Li, Phys. Rev. Lett. **76**, 4046 (1996).
[9] M. Pissas, G. Kallias, E. Devlin, A. Simopoulos, and D. Niarchos, J. Appl. Phys. **81**, 5770 (1997).
[10] V. Chechersky, A. Nath, I. Isaac, J. P. Franck, K. Ghosh, H. Ju, and R. L. Greene, Phys. Rev. B **59**, 497 (1999).
[11] J. M. De Tereza, C. Ritter, M. R. Ibarra, P. A. Algarabel, J. L. Garcia-Munoz, J. Blasco, J. Garcia, and C. Marquina, Phys. Rev. B **56**, 3317 (1997).
[12] J. A. Alonso, J. L. Martinez, M. J. Martinez-Lope, M. T. Casais, and M. T. Fernandez-Diaz, Phys. Rev. B **82**, 189 (1999).
[13] Guo-meng Zhao, H. Keller, and W. Pellier, J. Phys.: Condens. Matter **12**, L361 (2000).
[14] M. Itoh, I. Natori, S. Kubota, and K. Motoya, J. Phys. Soc. Jpn. **63**, 1486 (1994).
[15] D. N. H. Nam, K. Jonason, P. Nordblad, N. V. Khiem, and N. X. Phuc, Phys. Rev. B **59**, 4189 (1999).
[16] N. Gayathni, A. K. Raychandhuri, S. K. Tiwary, G. Gundakaram, A. Arulraj, and C. N. R. Rao, Phys. Rev. B **56**, 1345 (1997).
[17] J. R. L. de Almeida, J. Phys.: Condens. Matter **11**, L223 (1999).
[18] R. Laiho, K. G. Lisunov, E. Lähderanta, P. A. Petrenko, V. N. Stamov, and V. S. Zakhvalinskii, J. Magn. Magn. Mater. **213**, 271 (2000).
[19] R. Laiho, K. G. Lisunov, E. Lähderanta, P. A. Petrenko, J. Salminen, V. N. Stamov, and V. S. Zakhvalinskii, J. Phys.: Condens. Matter **12**, 5751 (2000).
[20] N. Moutis, I. Panagiotopulos, M. Pissas, and D. Niarchos, Phys. Rev. B **59**, 1129 (1999).
[21] Ch. V. Mohan, M. Seeger, H. Kronmuller, P. Murugaraj, and J. Maier, J. Magn. Magn. Mater. **183**, 348 (1998).
[22] J. Mira, J. Rivas, M. Vazques, J. M. Garcia-Beneyetz, J. Areas, R. D. Sanchez, and M. A. Senaris-Rodriguez, Phys. Rev. B **59**, 123 (1999).
[23] R. H. Heffner, J. E. Sonier, D. E. MacLaughlin, G. J. Nieuwenhnys, G. Ehlers, F. Mezei, S.-W. Cheong, J. S. Gardner, and H. Röder, Phys. Rev. Lett. **85**, 3285 (2000).
[24] P. C. Hohenberg and B. I. Halperin, Rev. Mod. Phys. **49**, 435 (1977).
[25] K. Eftimova, R. Laiho, E. Lähderanta, and P. Nordblad, J. Magn. Magn. Mater. **166**, 179 (1997).
[26] K. Jonason, J. Mattson, and P. Nordblad, Phys. Rev. B **53**, 6507 (1996).
[27] R. M. Roshko and W. Ruan, J. Magn. Magn. Mater. **104–107**, 1613 (1992).
[28] J. Mattsson, T. Jonsson, and P. Nordblad, Phys. Rev. Lett. **74**, 4305 (1995).
[29] J. L. Tholence, Physica B **126**, 157 (1984).
[30] K. Eftimova, E. Lähderanta, and R. Laiho, J. Phys.: Condens. Matter **11**, 6935 (1999).
[31] C. P. Bean and J. D. Livingston, J. Appl. Phys. **30**, 120S (1959).
[32] T. Jonsson, J. Mattsson, P. Nordblad, and P. Svedlindh, J. Magn. Magn. Mater. **168**, 269 (1997).